ACCOUNTS
of chemical research

Atomically Precise Gold Nanoclusters as New Model Catalysts

GAO LI AND RONGCHAO JIN*

Department of Chemistry, Carnegie Mellon University, 4400 Fifth Avenue, Pittsburgh, Pennsylvania 15213, United States

RECEIVED ON JULY 20, 2012

CONSPECTUS

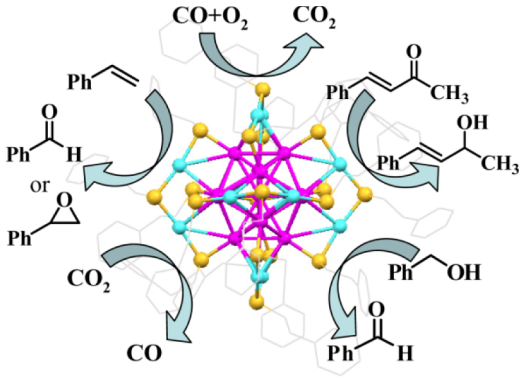

Many industrial catalysts involve nanoscale metal particles (typically 1−100 nm), and understanding their behavior at the molecular level is a major goal in heterogeneous catalyst research. However, conventional nanocatalysts have a nonuniform particle size distribution, while catalytic activity of nanoparticles is size dependent. This makes it difficult to relate the observed catalytic performance, which represents the average of all particle sizes, to the structure and intrinsic properties of individual catalyst particles. To overcome this obstacle, catalysts with well-defined particle size are highly desirable.

In recent years, researchers have made remarkable advances in solution-phase synthesis of atomically precise nanoclusters, notably thiolate-protected gold nanoclusters. Such nanoclusters are composed of a precise number of metal atoms (*n*) and of ligands (*m*), denoted as $Au_n(SR)_m$, with *n* ranging up to a few hundred atoms (equivalent size up to 2−3 nm). These protected nanoclusters are well-defined to the atomic level (i.e., to the point of molecular purity), rather than defined based on size as in conventional nanoparticle synthesis. The $Au_n(SR)_m$ nanoclusters are particularly robust under ambient or thermal conditions (<200 °C).

In this Account, we introduce $Au_n(SR)_m$ nanoclusters as a new, promising class of model catalyst. Research on the catalytic application of $Au_n(SR)_m$ nanoclusters is still in its infancy, but we use $Au_{25}(SR)_{18}$ as an example to illustrate the promising catalytic properties of $Au_n(SR)_m$ nanoclusters.

Compared with conventional metallic nanoparticle catalysts, $Au_n(SR)_m$ nanoclusters possess several distinct features. First of all, while gold nanoparticles typically adopt a face-centered cubic (fcc) structure, $Au_n(SR)_m$ nanoclusters (<2 nm) tend to adopt different atom-packing structures; for example, $Au_{25}(SR)_{18}$ (1 nm metal core, Au atomic center to center distance) has an icosahedral structure. Secondly, their ultrasmall size induces strong electron energy quantization, as opposed to the continuous conduction band in metallic gold nanoparticles or bulk gold. Thus, nanoclusters become semiconductors and possess a sizable bandgap (e.g., ∼1.3 eV for $Au_{25}(SR)_{18}$). In addition, $Au_n(SR)_m$ can be doped with a single atom of other metals, which is of great interest for catalysis, because the catalytic properties of nanoclusters can be truly tuned on an atom-by-atom basis.

Overall, atomically precise $Au_n(SR)_m$ nanoclusters are expected to become a promising class of model catalysts. These well-defined nanoclusters will provide new opportunities for achieving fundamental understanding of metal nanocatalysis, such as insight into size dependence and deep understanding of molecular activation, active centers, and catalytic mechanisms through correlation of behavior with the structures of nanoclusters. Future research on atomically precise nanocluster catalysts will contribute to the fundamental understanding of catalysis and to the new design of highly selective catalysts for specific chemical processes.

1. Introduction

Heterogeneous catalysis has a long history and dates back to the 19th century.[1] A central topic pertains to the preparation of highly active and selective catalysts for various chemical processes. Metal particles occupy an important position in heterogeneous catalysis. In terms of particle size, almost all the metal particle catalysts fall in the nanometer range (e.g., 1−100 nm); in particular, the 1−10 nm range is of critical importance for nanocatalysis.[2] The high activity of small particles is attributed to their high surface-to-volume ratio, surface geometric effect (e.g., surface atom arrangement and low-coordinated atoms), the electronic properties, and the quantum size effect. Understanding the atomic and molecular level details of reactant activation and

Published on the Web 03/27/2013 www.pubs.acs.org/accounts
10.1021/ar300213z

reaction steps on nanoparticle surfaces constitutes a major goal in heterogeneous catalysis research.

A heterogeneous catalyst consists of two components, the active metal nanoparticle and the support (e.g., oxide powders). The primary role of the support is to anchor nanoparticles on its surface, preventing the particles from sintering during the catalytic reaction. A traditional, popular method for making heterogeneous catalysts involves impregnation of oxide powders in a metal salt solution, followed by drying and calcination at high temperatures (e.g., 300−1000 °C).[3] Under high temperatures, the metal salt decomposes and converts to metal oxide particles (for active metals) or metallic particles (for noble metals) on the support. An apparent disadvantage of this method is the broad size distribution of particles on the support; undecomposed metal ions may also exist. Such heterogeneities pose major challenges to fundamental studies of catalysis, albeit from the viewpoint of practical catalysis these poorly controlled catalysts are still acceptable as long as the catalysts give rise to high activity, selectivity, and durability.

Toward the pursuit of fundamental mechanistic understanding of heterogeneous catalysis, well-defined catalysts have long been highly sought after. Single crystal surfaces were exploited as model catalysts back in the 1970s.[4,5] In the last decades, surface science has made a major impact on catalysis, and the knowledge obtained provides invaluable information toward rational catalyst design,[4−6] but the material and pressure gaps of model single-crystal surfaces have long been recognized, which raises questions whether the conclusions from single crystal surface studies are all transferable to the case of nanoscale catalysts. Another line of research focuses on mass-selected gas-phase clusters and soft deposition onto supports.[7,8] Additionally, catalysis by few-atom metal cluster complexes has also been pursued.[9,10] In recent years, solution-phase synthesis of monodisperse nanoparticles has achieved significant progress. A variety of uniform colloidal nanoparticles with excellent size and shape control have been achieved, and their catalytic properties have been investigated recently.[11−14]

In this Account, we focus on a new class of well-defined, ultrasmall metal nanoparticles (so-called nanoclusters).[15] The quantization effect leads to evolution of the continuous conduction band in metallic nanoparticles to discrete energy levels when the size is below ~2 nm.[16] Atomically precise nanoclusters (e.g., gold) with excellent size control have been obtained,[15,17] which will allow for precise measurements of size-dependent catalytic performance.[17] Moreover, total structures of nanoclusters can be solved by X-ray crystallography, which permits precise correlation between nanocluster structure and catalytic properties. Such well-defined nanocatalysts are expected to provide exciting opportunities for fundamental catalysis research. Below we first discuss briefly the synthesis and characterization of atomically precise nanoclusters using gold as a paradigm, then focus on the catalytic properties of nanocluster catalysts, including oxidation and hydrogenation reactions, as well as photo- and electrocatalysis.

2. Synthesis and Thermal Stability of Atomically Precise Nanoclusters

Solution-phase nanoclusters are typically protected by ligands. Herein, we concentrate on thiolate-protected gold nanoclusters (denoted as $Au_n(SR)_m$), which are particularly robust.

2.1. Size-Focusing Synthesis of Atomically Precise Nanoclusters. In our synthetic efforts,[18,19] we aimed at "one pot for one size" without necessitating chromatographic or gel separation. After years of efforts, we have successfully developed a universal methodology for bulk solution-phase synthesis of discrete-sized $Au_n(SR)_m$ nanoclusters with size control.[20] Details of the methodology have been discussed elsewhere.[20] Herein we only briefly describe the basic principle of the size-focusing methodology. In this method, a *proper* distribution of size-mixed nanoclusters is first made by kinetically controlling the reduction of gold precursor (typically salt) with $NaBH_4$; then the size-mixed nanoclusters are subjected to size-focusing under appropriate conditions (e.g., at 80 °C and in the presence of excess thiol), under which the not-so-stable nanoclusters decompose or convert to the stable size, and eventually only the most stable nanocluster in the distribution survives the "focusing" process (Figure 1), hence, survival of the most robust, much like "survival of the fittest". By adjustment of the initial size range through kinetic control in the first step, subsequent size-focusing gives rise to a series of size-discrete, robust $Au_n(SR)_m$ nanoclusters,[20,21] such as $Au_{25}(SR)_{18}$, $Au_{38}(SR)_{24}$, $Au_{144}(SR)_{60}$, and $Au_{333}(SR)_{79}$, all of which are of molecular purity.

Among the $Au_n(SR)_m$ nanoclusters, $Au_{25}(SR)_{18}$ has been extensively investigated for catalysis (*vide infra*). Herein we briefly discuss the structure and electronic properties.[16] The $Au_{25}(SR)_{18}$ structure comprises a 13-atom Au_{13} icosahedral core (Figure 2A, magenta portion) and a $Au_{12}(SR)_{18}$ shell (Figure 2A, cyan and yellow). From the space-filling model, one can see that the shell (or surface) Au atoms and even some of the icosahedral core Au atoms are accessible to reactant molecules in catalytic reactions (Figure 2B).

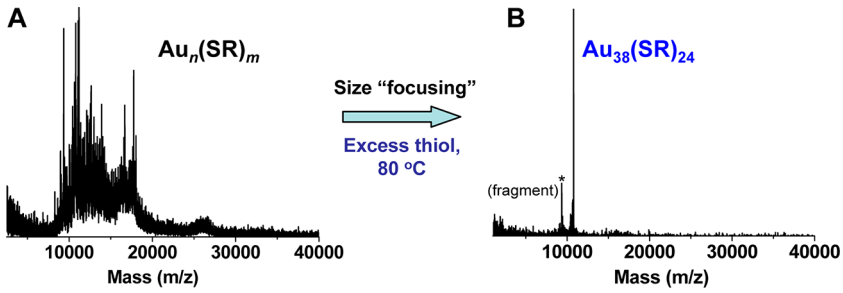

FIGURE 1. Synthesis of atomically precise nanoclusters (example, $Au_{38}(SCH_2CH_2Ph)_{24}$) via size-focusing of polydisperse nanoclusters.

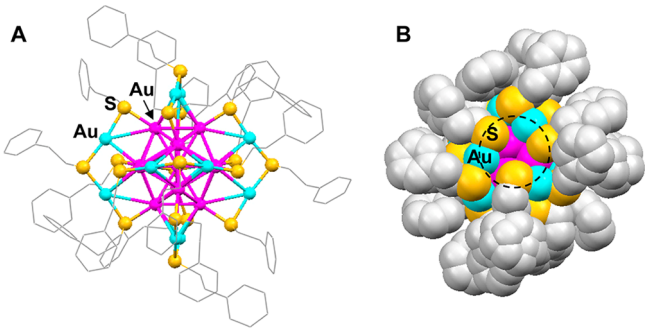

FIGURE 2. Structure of $Au_{25}(SCH_2CH_2Ph)_{18}$ nanoclusters (magenta, gold atoms of the core; cyan, gold atoms of the shell (or surface)). (A) ball-stick model; (B) space-filling model. Adapted with permission from ref 16.

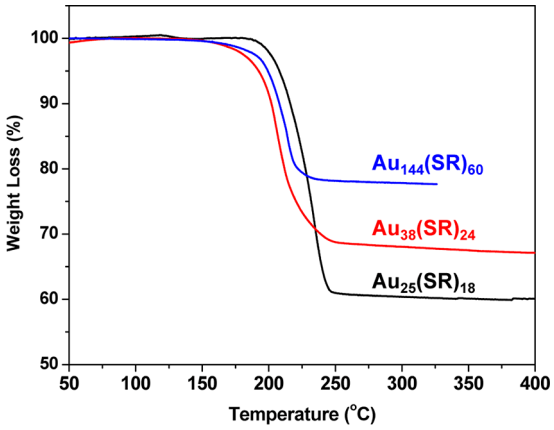

FIGURE 3. Thermogravimetric analysis of $Au_n(SR)_m$ nanoclusters. Adapted with permission from ref 25.

The cavities (or pocket-like sites) may serve as catalytically active centers. The electronic structure of $Au_{25}(SR)_{18}$ exhibits discrete energy levels caused by the quantum-size effect. The molecular orbitals can be *roughly* divided into the Au-core orbitals (i.e., primarily contributed by Au_{13}) and the shell orbitals (i.e., primarily by $Au_{12}(SR)_{18}$), reflecting the geometric core–shell structure.[15,16] For other types of thiolate-protected $Au_{25}(SR)_{18}$ (e.g., SR = SC_6H_{13}, $SC_{12}H_{25}$, glutathione (SG)), we have proven that the same geometric structure is retained in all $Au_{25}(SR)_{18}$ regardless of the thiolate type.[22] Additionally, all the $Au_{25}(SR)_{18}$ nanoclusters show the identical optical absorption spectrum.[19,23] For $Au_{38}(SR)_{24}$, the structure comprises a bi-icosahedral Au_{23} core and six $Au_2(SR)_3$ and three $Au(SR)_2$ staple motifs for protecting the core.[24] Crystallization of $Au_{144}(SR)_{60}$ has not been successful thus far.

2.2. Thermal Stability. The thermal stability of $Au_n(SR)_m$ nanoclusters is important for catalytic applications since most reactions are run under thermal conditions. Thermogravimetric analysis (TGA) shows that $Au_n(SR)_m$ starts to lose ligands at ~200 °C and ligand desorption completes at ~250 °C in N_2 atomosphere (Figure 3).[25] The thermal decomposition is not affected by the atmosphere (e.g., N_2, air, O_2, or H_2). With respect to the aqueous-soluble $Au_{25}(SG)_{18}$ nanocluster, the onset temperature of ligand desorption is also at ~200 °C but the completion temperature is higher (~300 °C) due possibly to the strong hydrogen-bonding interactions between –SG ligands.

3. Reactivity and Catalytic Properties of $Au_n(SR)_m$ Nanoclusters

According to the afore-discussed TGA results of $Au_n(SR)_m$ nanoclusters, if ligands-on catalysts are desired in catalytic reactions, the operation temperature should not exceed 200 °C; on the other hand, if ligands-off catalysts are preferred, one can pretreat the catalyst at 250–300 °C to remove the ligands and expose the entire cluster to reactants.

3.1. Interaction between Nanoclusters and O_2. In catalysis, O_2 activation is of major interest since O_2 is used in many oxidation reactions.[2,26] We found that $Au_{25}(SR)_{18}$ can interact with O_2 even at room temperature, though the reaction is slow (on the order of days).[27] The native $Au_{25}(SR)_{18}$ nanocluster is anionic (i.e., $[Au_{25}(SCH_2CH_2Ph)_{18}]^-$, counterion = tetraoctylammonium (TOA^+)). When a solution of $[Au_{25}(SCH_2CH_2Ph)_{18}]^-$ was exposed to air, a discernible color change was observed, which was also reflected in the UV–vis spectra (Figure 4). The product was determined to be charge-neutral $[Au_{25}(SCH_2CH_2Ph)_{18}]^0$.[27] This result is quite interesting, as one would expect that O_2 should first

oxidize the thiol ligands, as is the case of thiol self-assembled monolayers on bulk gold surfaces, but our results revealed that the gold core, instead of the ligands, first undergoes one-electron loss.[15] Single-crystal X-ray crystallographic analysis[27] revealed that the $[Au_{25}(SCH_2CH_2Ph)_{18}]^0$ structure shares the same framework as that of $[Au_{25}(SCH_2CH_2Ph)_{18}]^-$. The negative charge of $[Au_{25}(SCH_2CH_2Ph)_{18}]^-$ resides within the Au_{13} core of the cluster.[15] The redox process between $[Au_{25}(SCH_2CH_2Ph)_{18}]^0$ and $[Au_{25}(SCH_2CH_2Ph)_{18}]^-$ is completely reversible. Using peroxide as the oxidant, the anion-to-neutral conversion is much faster than using O_2. The oxidation by O_2 or peroxide was also observed in the water-soluble $Au_{25}(SG)_{18}$ nanocluster. Both the organic-soluble and aqueous $Au_{25}(SR)_{18}$ (where SR = SCH_2CH_2Ph, SC_6H_{13} or SG) have been utilized in catalytic work.

3.2. Catalytic Oxidation. The reversible charge-state conversion of $[Au_{25}(SR)_{18}]^q$ indicates that the nanocluster can be utilized in catalytic oxidation or reduction reactions.

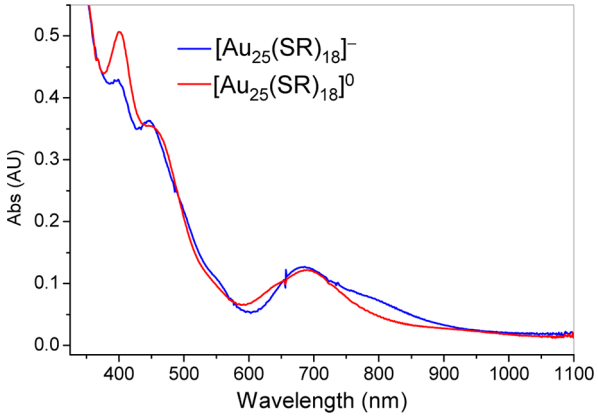

FIGURE 4. Reversible conversion between $[Au_{25}(SR)_{18}]^0$ and $[Au_{25}(SR)_{18}]^-$. Adapted with permission from ref 27.

3.2.1. Catalytic Oxidation of CO to CO_2. We first discuss CO oxidation. This reaction has been extensively investigated in gold catalysis.[2,28] The gold catalysts in the literature are typically prepared from gold salts through methods of impregnation, coprecipitation, deposition–precipitation, etc.[2] The TiO_2-supported gold catalyst is generally identified to be the most effective catalyst. With ligand-protected gold nanocluster catalysts, Nie et al.[29] found surprisingly that the $Au_{25}(SR)_{18}/TiO_2$ catalyst had no catalytic activity even up to 200 °C (Figure 5A), whereas $Au_{25}(SR)_{18}/CeO_2$ exhibited moderate activity (onset temperature ~60 °C). These results imply that some striking differences exist between conventional Au(bare)/TiO_2 catalysts[28] and ligands-on $Au_{25}(SR)_{18}/TiO_2$ catalyst.[29]

Significantly, pretreatment of the $Au_{25}(SR)_{18}/CeO_2$ catalyst in O_2 for 1.5–2 h at 150 °C (T_{pre}) led to a drastic increase in catalytic activity (onset temperature shifted to rt), Figure 5B, and complete CO conversion was reached at reaction temperature (T_{rxn}) ~100 °C. Prolonged O_2 pretreatment at 150 °C (e.g., >2 h) did not lead to further enhancement in catalytic activity (Figure 5B); neither does the increase in T_{pre} to 250 °C (above the thiolate desorption) further increase the catalytic activity. The presence of water vapor in the feed gases exhibited a promotion effect on the catalyst performance in the 40–100 °C reaction temperature range; above 100 °C the conversion of CO to CO_2 was already complete, so the effect of vapor was not manifested. In the case of feed gas that contains vapor, O_2 pretreatment at even lower temperature (e.g., T_{pre} = 100 °C) could lead to the same drastic enhancement in activity.[29]

The drastic effect of thermal O_2 pretreatment of the $Au_{25}(SR)_{18}/CeO_2$ catalyst was surprisingly not observed in $Au_{25}(SR)_{18}/TiO_2$. For the latter, we even performed thermal

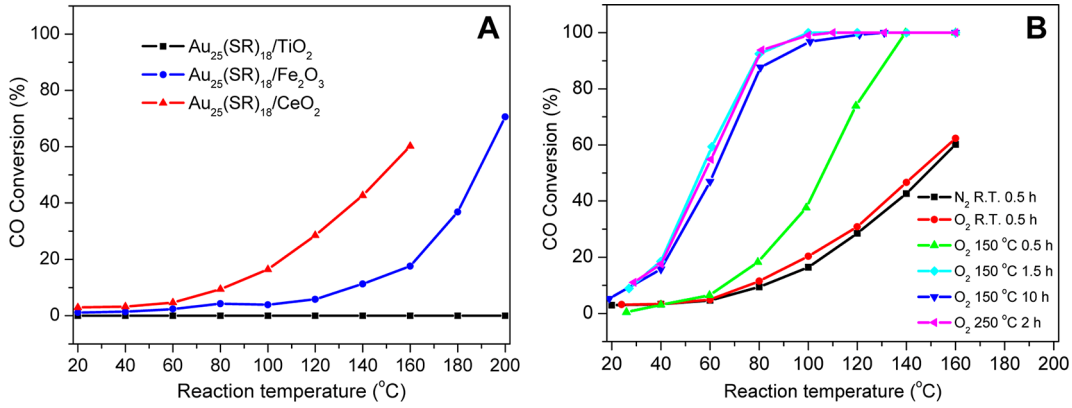

FIGURE 5. (A) Catalytic activity of different oxide-supported $Au_{25}(SR)_{18}/MO_x$ catalysts for CO oxidation. Catalyst pretreatment condition, N_2 at room temperature (rt) for 0.5 h; reaction conditions, GHSV ≈ 7500 mL g^{-1} h^{-1}, catalyst, 0.1 g total. (B) Catalytic activity of $Au_{25}(SR)_{18}/CeO_2$ after different pretreatments. Adapted with permission from ref 29.

SCHEME 1. Proposed CO Oxidation at the Perimeter Sites of $Au_{25}(SR)_{18}/CeO_2$

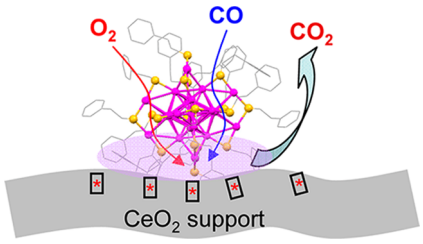

pretreatment up to 250 °C in O_2 atmosphere, but only a small increase in catalytic activity was observed (with or without H_2O vapor in the feed gas). In addition, thermal pretreatment of the catalysts in N_2 (as opposed to O_2) did not give rise to the above drastic effect in *all* catalysts. Thus, O_2 is critical and might be converted to certain active species on the catalysts during the pretreatment process. Characterization of the $Au_{25}(SR)_{18}/CeO_2$ catalyst implied that the ligands remained on the cluster after the 150 °C pretreatment in O_2. Our results indicate that the interface between $Au_{25}(SR)_{18}$ and CeO_2 appears critical and the reaction may occur at the perimeter sites.[30] Our rough picture (Scheme 1) is that O_2 should first convert to O_2^- by withdrawing an electron from the cluster; then it migrates to the cluster/CeO_2 interface and converts to hydroperoxide species on CeO_2. The gold-activated CO should be oxidized at the perimeter sites of the catalyst. In future work, it is intriguing to look into several issues, including (i) the unique role of CeO_2 (versus TiO_2), (ii) the true nature of the active oxygen species, and (iii) the interactions between $Au_{25}(SR)_{18}$ and the support.

3.2.2. Selective Oxidation of Styrene. Zhu et al.[31] investigated solution-phase styrene oxidation with O_2 catalyzed by $Au_{25}(SR)_{18}$ nanoclusters (in the form of free clusters in solution or being supported on oxides). The reaction was performed at 80−100 °C for 12−24 h (toluene as solvent), producing benzaldehyde as the major product (selectivity ∼70%) and styrene epoxide (less, selectivity ∼25%) and minor byproduct acetophenone (selectivity ∼5%).

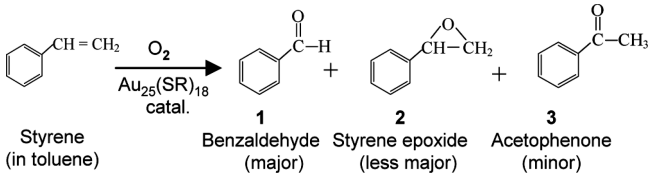

A 35% conversion of styrene was obtained even with a part per million level of catalysts in solution. For SiO_2-supported $Au_{25}(SR)_{18}$ (without calcination pretreatment), the catalyst gave rise to comparable performance as that of the unsupported catalyst. The advantage of supported

SCHEME 2. Epoxidation of Styrene Catalyzed by Ligands-Off Au_{25}/HAP Catalyst[a]

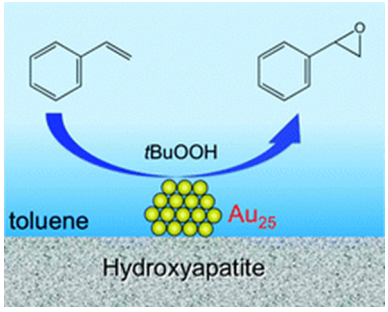

[a]Adapted with permission from ref 32.

$Au_{25}(SR)_{18}/SiO_2$ is that the nanoclusters are more durable and the catalyst can be readily recycled for reuse in catalytic reaction. No apparent deterioration in activity and selectivity of the reused supported catalyst was observed after multiple cycles.[31]

Liu et al.[32] investigated $Au_{25}(SG)_{18}$/HAP catalyst (where HAP refers to hydroxyapatite, $Ca_{10}(PO_4)_6(OH)_2$) for selective oxidation of styrene. After removing ligands by 300 °C thermal treatment, the resultant ligands-off Au_{25}/HAP catalyst preserved the Au_{25} size but might have had a different structure.[32] The catalyst was found to catalyze styrene oxidation (with anhydrous *tert*-butyl hydroperoxide (TBHP) as the oxidant), and the reaction yielded styrene oxide as the major product at 80 °C in toluene (Scheme 2). High yield of styrene oxide (∼92% at 12 h reaction time) was obtained, which is much higher than conventional nanocatalysts (ca. 50−60% yield) with the same Au loading (0.5 wt %). They further commented that toluene (solvent) was essential for obtaining high yield of styrene oxide and other important factors included the use of anhydrous toluene and TBHP for enhancing the yield of styrene oxide.

Zhu et al.[25] also investigated three oxidant systems: (a) TBHP as the oxidant; (b) TBHP as the initiator and O_2 as the main oxidant; (c) O_2 as the oxidant (without initiator). Since TBHP is quite reactive, the reaction with TBHP catalyzed by $Au_{25}(SR)_{18}/SiO_2$ (no calcination pretreatment) gave high conversion of styrene (e.g., 86%) with ∼100% selectivity for benzaldehyde. System b showed much lower activity (25% conversion of styrene, ∼100% selectivity for benzaldehyde), and system c (solely O_2) was even lower in activity (18% conversion and 80% selectivity for benzaldehyde). A similar order of activity was also found for $Au_{38}(SR)_{24}/SiO_2$ and $Au_{144}(SR)_{60}/SiO_2$ catalysts in these three oxidant systems.[25] The results indicate that the ingredients of the oxidant play a critical role in the reaction and that O_2 activation is a key step for achieving high conversion

of styrene. The results also imply that the active oxygen species in the catalytic cycles may be peroxide- or hydroperoxide-like species.

The above results of catalytic styrene oxidation by $Au_n(SR)_m$ allow us to gain some valuable atomic level insight. The Au_{13} core of $Au_{25}(SR)_{18}$ possesses eight (when $q = -1$) or seven (when $q = 0$) delocalized valence electrons, which originate from Au(6s) and are primarily distributed within the Au_{13} core,[15] while the Au_{12} shell bears positive charges ($\delta+$) due to charge transfer to sulfur atoms of the ligands. We believe that the electron-rich Au_{13} core facilitates O_2 activation by electron donation to O_2, accompanied by $[Au_{25}(SR)_{18}]^-$ conversion to neutral $[Au_{25}(SR)_{18}]^0$; note that this oxidation readily occurs at elevated temperatures (e.g., under catalytic reaction conditions). A similar O_2 activation mechanism via electron transfer was also identified in PVP-protected gold nanoclusters for aerobic alcohol oxidation.[17] For styrene oxidation on $Au_{25}(SR)_{18}$, activation of the C=C bond of styrene should be facilitated by the partial positive charge[33] ($Au^{\delta+}$, $\delta = \sim 0.3$) on the surface gold atoms. Theoretical work is still needed to obtain deeper understanding of the adsorption geometry and the structure of intermediates.

3.2.3. Aerobic Oxidation of Cyclohexane. Tsukuda and co-workers[34] made HAP-supported $Au_{10}(SG)_{10}$, $Au_{18}(SG)_{14}$, $Au_{25}(SG)_{18}$, and $Au_{39}(SG)_{24}$ nanocluster catalysts with 0.2 wt % loading of clusters; note that the cluster structures (except Au_{25}) are not known yet. Optical reflectance spectroscopy and TEM measurements confirmed that the $Au_n(SG)_m$ clusters adsorbed on HAP were intact. Subsequent thermal calcination at 300 °C for 2 h in vacuo completely removed the −SG ligands on the clusters. TEM analysis showed no growth of the ligands-off clusters into large plasmonic nanoparticles, which is attributed to the excellent protecting role of HAP (i.e., its relatively strong interaction with clusters via the PO_4^{3-} moiety).[32] It should be noted that TEM cannot measure the precise number of Au atoms in the resultant ligands-off Au_n clusters (originally $n = 10$, 18, 25, and 39) on HAP, but one still obtained the ligands-off catalysts with an unprecedented atomic level control.[17,34] The catalytic performance of these ligands-off Au_n/HAP catalysts for the oxidation of cyclohexane was evaluated using O_2 as the oxidant (under 1 MPa and solvent-free conditions at 150 °C). Cyclohexanol and cyclohexanone were obtained as the primary products with nearly equal yields; no adipic acid was formed in the reaction. The total selectivity (cyclohexanone and cyclohexanol) was very high (~99%), and interestingly the turnover frequency (TOF) values exhibited an optimal cluster size around $n \approx 40$ (Figure 6).[34]

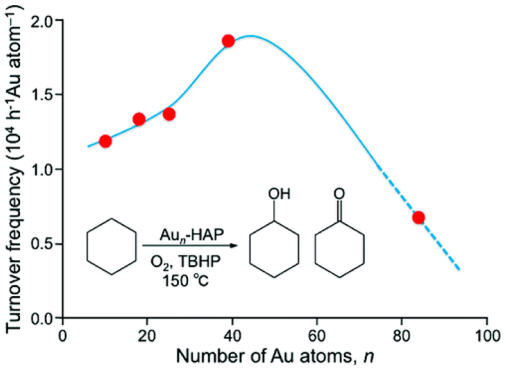

FIGURE 6. Selective oxidation of cyclohexane to cyclohexanol and cyclohexanone with O_2 as the oxidant catalyzed by ligands-off Au_n/HAP. Adapted with permission from ref 34.

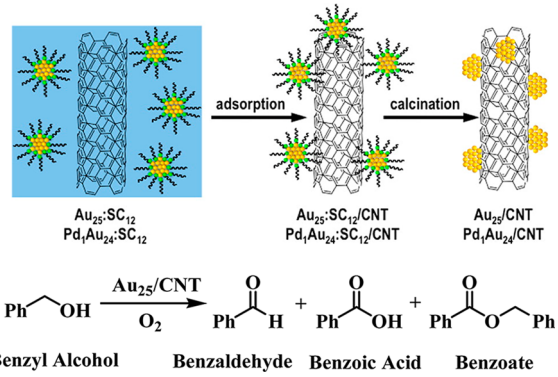

FIGURE 7. Au_{25}/CNT and Pd_1Au_{24}/CNT catalysts for benzyl alcohol oxidation. Adapted with permission from ref 35.

3.2.4. Aerobic Oxidation of Alcohol. Xie et al.[35] prepared carbon nanotube (CNT)-supported Au_{25} and single-palladium-doped Pd_1Au_{24} nanocluster catalysts via deposition of $Au_{25}(SC_{12}H_{25})_{18}$ and $Pd_1Au_{24}(SC_{12}H_{25})_{18}$, respectively, followed by calcination to remove ligands. In the aerobic oxidation of benzyl alcohol (Figure 7), Pd_1Au_{24}/CNT showed significantly enhanced activity (74% conversion of $PhCH_2OH$) compared with Au_{25}/CNT (22% conversion). The effect of single-Pd-atom replacement is remarkable. This doping effect was ascribed to the modulation of the electronic structures of the cluster by intracluster electron transfer from Pd to Au.[35]

3.3. Catalytic Hydrogenation. Besides the oxidation reactions, $Au_n(SR)_m$ nanocluster catalysts were also demonstrated to be capable of catalyzing hydrogenation reactions in solution phase,[31,36] such as chemoselective hydrogenation of α,β-unsaturated ketones to α,β-unsaturated alcohols under mild conditions (60 °C, in mixed solvents (1:1 toluene/acetonitrile)).[31] The $Au_{25}(SR)_{18}$ clusters were found

to hydrogenate preferentially the C=O bond of benzalacetone against the C=C bond, and the C=O hydrogenated product (i.e., unsaturated alcohol) was obtained with 76% selectivity, with 14% selectivity for saturated ketone and 10% for saturated alcohol.[31] A nearly complete selectivity for α,β-unsaturated alcohol was further obtained in a mixed toluene/ethanol (1:1) solvent after optimization.[36]

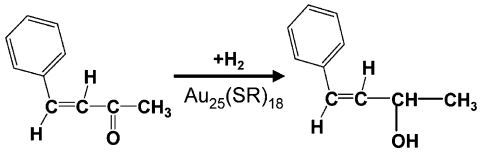

Kawasaki and co-workers[37] compared the catalytic properties of $Au_{25}(SG)_{18}$ nanoclusters and *N,N*-dimethylformamide (DMF)-stabilized gold clusters (size unidentified) in the reduction reaction of 4-nitrophenol (PNP) to 4-aminophenol by $NaBH_4$. The $Au_{25}(SG)_{18}$ nanoclusters exhibited higher catalytic activity than DMF-capped clusters in the PNP reduction at 298 K (the pseudo-first-order rate constant $k_{app} = 8 \times 10^{-3}$ s^{-1} for $Au_{25}(SG)_{18}$ versus 3×10^{-3} s^{-1} for DMF-capped Au clusters). High activity was obtained even with as low catalyst concentration as 1.0 μM. No induction time was observed despite −SG being a strongly binding ligand, while the DMF-stabilized Au clusters exhibited an induction time, which was attributed to the impedance by the surface DMF layer on the clusters when reactants accessed the cluster surface.[37] For $Au_{25}(SG)_{18}$ clusters, the unique core−shell structure seems to pose less steric hindrance and thus renders the catalytically active surface sites more accessible to reactants. Scott and co-workers recently demonstrated intact $Au_{25}(SR)_{18}$ clusters for the reduction of 4-nitrophenol by $NaBH_4$, and the high stability under the reaction conditions enabled the recyclability of these clusters.[38]

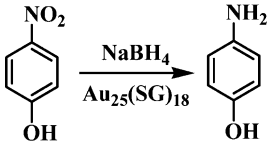

3.4. Photocatalysis by Gold Nanoclusters. Tatsuma and co-workers studied the photocatalytic properties of $Au_{25}(SG)_{18}$ nanoclusters.[39,40] The carboxylic group of −SG ligands facilitates adsorption of the clusters to the TiO_2 electrode surface. Studies showed that the photoexcited electrons in $Au_{25}(SG)_{18}$ can be injected into the TiO_2 conduction band with a ~60% internal quantum yield.[39] Visible light-driven photocatalysis by Au_{25}-modified TiO_2 was investigated for photooxidation of phenol derivates and ferrocyanide and reduction of Ag^+, Cu^{2+}, and dissolved oxygen.[40]

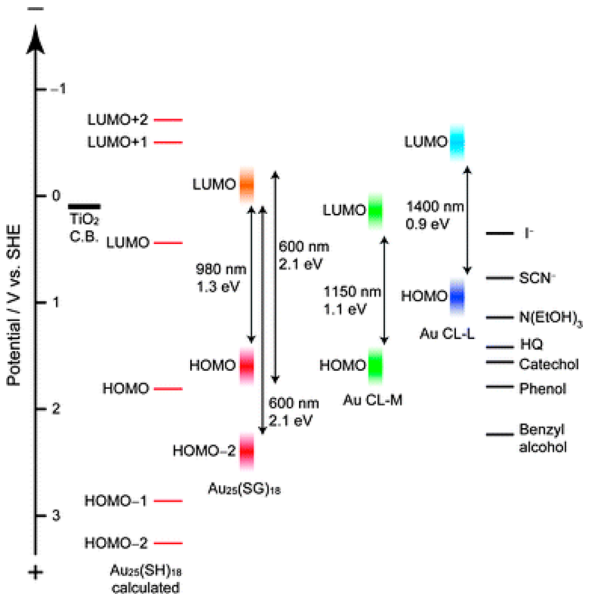

FIGURE 8. Energy level diagram of $Au_{25}(SG)_{18}$, $Au_{38}(SG)_{24}$ (Au CL-M), and larger ones (Au CL-L). Adapted with permission from ref 41.

Photocatalysis based on the excitation of $Au_{25}(SG)_{18}$ (as sensitizer) was even observed under near-IR light (λ = 860 nm). Larger $Au_n(SG)_m$ nanoclusters with core diameter up to 1.6 nm were also studied.[41] The photocurrent responses of cluster-modified TiO_2 electrodes in the presence of various electron donors allowed an estimation of electron levels such as HOMO and LUMO levels (Figure 8). It was found that the potential of the occupied levels involved in photoinduced charge separation shifts negatively as the cluster size increases.[41] Small Au clusters, such as $Au_{25}(SG)_{18}$, give rise to large photocurrents and are suitable for oxidizing a variety of donors, while large clusters are suitable for selective oxidation of donors with negative redox potentials.

In another study, Lee et al.[42] prepared $Au_{25}(SG)_{18}/TiO_2$ composites, in which clusters serve as cocatalyst, and investigated the photocatalytic activity for degradation of Uniblue A (UBA), but the as-prepared catalyst without removing ligands exhibited no enhancement by $Au_{25}(SG)_{18}$. After thermal treatment at 250 °C, the glutathione ligands on the cluster surface were removed partially (note: complete removal at 300 °C), and the photocatalytic activity of the composites was found to increase significantly. When compared with the afore-discussed reduction reaction of 4-nitrophenol[37,38] catalyzed by $Au_{25}(SR)_{18}$ as well as the CO oxidation[29] by $Au_{25}(SR)_{18}/CeO_2$, the different effects of the presence/absence of ligands raise an interesting question: to what extent do the ligands influence the catalytic reactions,

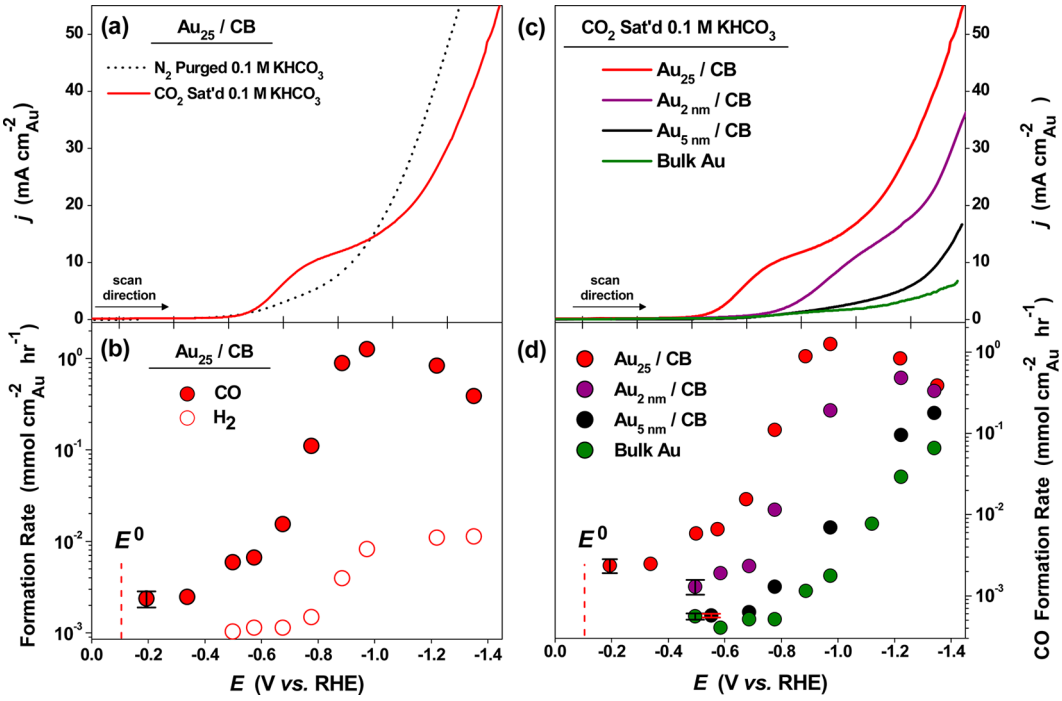

FIGURE 9. Electrochemical reduction of CO_2 in 0.1 M $KHCO_3$. (a) Linear sweep voltammograms (LSVs) of carbon black (CB)-supported $Au_{25}(SR)_{18}$ in N_2 purged (pH = 9) and CO_2 saturated (pH = 7) 0.1 M $KHCO_3$. (b) Potential dependent H_2 and CO formation rates for $Au_{25}(SR)_{18}$/CB. (c) LSVs of various Au catalysts in CO_2 saturated 0.1 M $KHCO_3$. (d) Potential-dependent CO formation rates for the various Au catalysts. Adapted with permission from ref 45. All Au_{25} in the panels refer to $Au_{25}(SR)_{18}$.

beneficially or adversely? Future experiments will reveal more insight into this issue.

3.5. Electrocatalysis by Gold Nanoclusters. 3.5.1. Electroreduction of O_2. Chen et al.[43] investigated ligand-protected Au_{25} and larger clusters for electrochemical reduction of O_2. In fuel cells, the sluggish reaction of oxygen reduction at the Pt cathode needs to be improved prior to practical applications. Chen et al. found that the electrocatalytic activity of Au nanoclusters for oxygen reduction exhibited a strong size dependence, reflected in the onset potential and peak current density; the smaller cluster exhibited higher electrocatalytic activity.[43] Compared with other electrocatalysts (without ligands), the appreciable voltammetric currents detected with the protected nanoclusters suggest that O_2 can readily access the particle surface and the presence of ligands does not impede the interfacial charge transfer.

3.5.2. Electroxidation Catalyzed by Nanoclusters. Kumar et al. evaluated $Au_{25}(SG)_{18}$ as an electrochemical oxidation catalyst.[44] The $Au_{25}(SG)_{18}$-modified electrode showed excellent electrocatalytic activity toward the oxidation of ascorbic acid and dopamine over a wide linear range from 0.71 to 44.4 μM. Moreover, pH-dependent electrocatalytic activity was observed, which was attributed to the consequence of pH-dependent electrostatic attraction/repulsion between the charged $Au_{25}(SG)_{18}$ clusters and the charged analytes. On the basis of the selective electroxidation, they further developed an amperometric sensing method for some compounds.[44]

3.5.3. Electroreduction of CO_2 to CO. Kauffman et al.[45] studied the interaction between CO_2 and $Au_{25}(SCH_2CH_2Ph)_{18}$ in solution. When the $Au_{25}(SR)_{18}$ solution (DMF as solvent) was saturated with CO_2, the optical absorbance features all exhibited discernible changes that are consistent with the increase in oxidation state of $Au_{25}(SR)_{18}$. Additionally, the photoluminescence maximum also showed an increase and blue shift.[45] The CO_2-induced optical changes can be reversed simply by purging the solution with N_2 to remove CO_2. The observed interaction between $Au_{25}(SR)_{18}$ and CO_2 was somewhat unexpected, because CO_2 shows little electronic interaction with traditional gold surfaces. DFT calculations revealed that the stable adsorption configuration of CO_2 consists of CO_2 interacting with three S atoms in the shell of the cluster. These interesting results prompted a study on the CO_2 electrochemical reduction with $Au_{25}(SR)_{18}$ as a catalyst. The electrocatalytic activity of $Au_{25}(SR)_{18}$ (supported on carbon black) for CO_2 reduction in aqueous 0.1 M $KHCO_3$ gave rise to CO formation at an onset potential of -0.193 V vs RHE. Remarkably, the onset of CO

fomation was within 90 mV of the $CO_2 \rightarrow CO$ formal potential (−0.103 V vs. RHE), Figure 9a,b. Compared with the larger Au catalysts (Figure 9c,d), $Au_{25}(SR)_{18}$ exhibited a large improvement (~300 mV), and the catalyst remains intact during the reaction.[45] Future work should explore the conversion of CO_2 to fuels catalyzed by nanoclusters.

3.6. Size Dependence of $Au_n(SR)_m$ Nanoclusters. While much work on $Au_{25}(SR)_{18}$ nanoclusters has been carried out for catalysis, other sized nanoclusters such as $Au_{38}(SR)_{24}$ and $Au_{144}(SR)_{60}$ have not been exploited to the same extent as $Au_{25}(SR)_{18}$. In terms of the size-dependent catalytic activities of $Au_n(SR)_m$ nanoclusters, Yan et al.[25] investigated the cluster size effect in styrene oxidation and observed the general order of activity: $Au_{25}(SR)_{18} > Au_{38}(SR)_{24} > Au_{144}(SR)_{60}$, that is, the smaller nanoclusters are more efficient than larger ones (per number of clusters or per unit surface area), especially when O_2 is used as the oxidant, because larger nanoclusters have lower O_2-activating capability, while TBHP can be readily activated even on large clusters; hence, no strong size dependence was observed.[25] Tsukuda and co-workers[34] found a volvano-type size dependence in the oxidation of cyclohexane using Au_n/HAP catalysts. The different size dependences observed[25,34,43] may be reaction-specific. Future work may explore further the size dependence, including both activity and selectivity.

4. Future Perspective: Atomic Level Control of Nanocatalysts

The atomically precise nanoclusters are expected to provide exciting opportunities for achieving some fundamental understanding of metal nanocatalysis. Correlation of catalytic properties of nanoparticles with their atomic level structure constitutes the ultimate goal in catalytic research. In this regard, well-defined nanocatalysts are expected to play signficant roles in unraveling fundamentals of catalysis. The well-defined $Au_n(SR)_m/MO_x$ nanocatalysts are expected to mediate the knowledge gap between single-crystal model catalysts and real-world nanocatalysts.

The ultrasmall size of $Au_n(SR)_m$ nanoclusters gives them nonmetallic electronic properties, manifested in the quantized electron energy levels. It is of particular interest to obtain insight into the effects of size-induced electron energy quantization on the catalytic properties. The properties of quantum-sized nanoclusters are very sensitive to the number of atoms in the cluster.[15] Significant changes may be induced by merely adding or removing one gold atom (cf., $Au_{25}(SR)_{18}$ versus $Au_{24}(SR)_{20}$).[16,46] Thus, nanocluster catalysts will allow one to truly tune the catalytic properties on an atom-by-atom basis. Moreover, the ligand-protected metal nanoclusters provide an opportunity for exerting the influence of surface ligands on catalytic reaction; for example, Zhu et al.[47] found the diastereoselective catalytic capability of $Au_{25}(SR)_{18}$ nanocluster catalyst was related to the −R group (e.g., phenylethyl vs longchain alkyl). On the other hand, strategies on removing surface ligands without causing size enlargement should be devised in future work, and structural characterization after ligand removal should be pursued.

The core−shell geometric structure of $Au_n(SR)_m$ nanoclusters[15] creates a unique environment (e.g., cavity sites) for activation of reactants. The copresence of the electron-rich core and the electron-deficient shell and the interplay between them[48] may be quite unique in activating reactants. On the basis of the $Au_n(SR)_m$ structures, future experiment in combination with theory may ultimately provide atomic level insight into molecular activation, structure−property relationship, and catalytic mechanisms.[11,17,49,50] Another interesting issue is to compare the catalysis by $Au_n(SR)_m$ and homogeneous Au(I) catalysts.

Finally, identification of the catalytically active sites is certainly a grand challenge and of fundamental significance. The nature of the catalytic active sites has intrigued researchers for many decades. However, without well-defined nanocatalysts, it would not be possible to pinpoint the active sites. Future research is expected to achieve advances in revealing the nature and structure of active sites. The steady advances in understanding the fundamentals of nanocatalysis will also lead to new design of highly selective catalysts under mild reaction conditions for chemical processes of energy and environmental importance.

We are grateful for support by the Chemical Sciences, Geosciences and Biosciences Division, Office of Basic Energy Sciences, Office of Science, U.S. Department of Energy, under Contract DE-FG02-12ER16354 and by the Air Force Office of Scientific Research (AFOSR) under Award No. FA9550-11-1-9999 (FA9550-11-1-0147).

BIOGRAPHICAL INFORMATION

Gao Li received his Ph.D. from Shanghai Jiao Tong University in 2011. He is currently a postdoctoral researcher at Carnegie Mellon University (CMU). His current research interests focus on preparation and catalytic applications of gold nanoclusters.

Rongchao Jin is an Associate Professor of Chemistry at CMU. He received his Ph.D. in Chemistry from Northwestern University in 2003. After three years of postdoctoral research at the University of Chicago, he joined the chemistry faculty of CMU in 2006.

His current research interests focus on atomically precise nanoparticles and their applications in catalysis, optics, and sensing.

FOOTNOTES

The authors declare no competing financial interest.

REFERENCES

1 Thomas, J. M.; Thomas, W. J. *Principles and Practices of Heterogeneous Catalysis*; Wiley: New York, 1996.

2 Bond, G. C.; Louis, C.; Thompson, D. T. *Catalysis by Gold*; Imperial College Press: London, 2006.

3 Jin, R.; Chen, Y.; Li, W.; Cui, W.; Ji, Y.; Yu, C.; Jiang, Y. Mechanism for Catalytic Partial Oxidation of Methane to Syngas over a Ni/Al_2O_3 Catalyst. *Appl. Catal., A* **2000**, *201*, 71–80.

4 Ertl, G. Reactions at Surfaces: From Atoms to Complexity (Nobel Lecture). *Angew. Chem., Int. Ed.* **2008**, *47*, 3524–3535.

5 Somorjai, G. A.; Park, J. Y. Concepts, Instruments, And Model Systems That Enabled the Rapid Evolution of Surface Science. *Surf. Sci.* **2009**, *603*, 1293–1300.

6 Han, P.; Axnanda, S.; Lyubinetsky, I.; Goodman, D. W. Atomic-Scale Assembly of a Heterogeneous Catalytic Site. *J. Am. Chem. Soc.* **2007**, *129*, 14355–14361.

7 Heiz, U., Landman, U., Eds. *Nanocatalysis*; Springer: New York, 2007.

8 Kaden, W. E.; Kunkel, W. A.; Kane, M. D.; Roberts, F. S.; Anderson, S. L. Size-Dependent Oxygen Activation Efficiency over $Pd_n/TiO_2(110)$ for the CO Oxidation Reaction. *J. Am. Chem. Soc.* **2010**, *132*, 13097–13099.

9 Gates, B. C. Supported Metal Clusters: Synthesis, Structure, and Catalysis. *Chem. Rev.* **1995**, *95*, 511–522.

10 Kulkarni, A.; Lobo-Lapidus, R. J.; Gates, B. C. Metal Clusters on Supports: Synthesis, Structure, Reactivity, and Catalytic Properties. *Chem. Commun.* **2010**, *46*, 5997–6015.

11 Jin, R. The Impacts of Nanotechnology on Catalysis by Precious Metal Nanoparticles. *Nanotechnol. Rev.* **2012**, *1*, 31–56.

12 Li, Y.; Liu, Q.; Shen, W. Morphology-Dependent Nanocatalysis: Metal Particles. *Dalton Trans.* **2011**, *40*, 5811–5826.

13 Chen, J. Y.; Lim, B.; Lee, E. P.; Xia, Y. N. Shape-Controlled Synthesis of Platinum Nanocrystals for Catalytic and Electrocatalytic Applications. *Nano Today* **2009**, *4*, 81–95.

14 Somorjai, G. A.; York, R. L.; Butcher, D.; Park, J. Y. The Evolution of Model Catalytic Systems; Studies of Structure, Bonding and Dynamics from Single Crystal Metal Surfaces to Nanoparticles, and from Low Pressure ($< 10^{-3}$ Torr) to High Pressure ($> 10^{-3}$ Torr) to Liquid Interfaces. *Phys. Chem. Chem. Phys.* **2007**, *9*, 3500–3513.

15 Qian, H.; Zhu, M.; Wu, Z.; Jin, R. Quantum Sized Gold Nanoclusters with Atomic Precision. *Acc. Chem. Res.* **2012**, *45*, 1470–1479.

16 Zhu, M.; Aikens, C. M.; Hollander, F. J.; Schatz, G. C.; Jin, R. Correlating the Crystal Structure of A Thiol-Protected Au_{25} Cluster and Optical Properties. *J. Am. Chem. Soc.* **2008**, *130*, 5883–5885.

17 Tsukuda, T. Toward an Atomic-Level Understanding of Size-Specific Properties of Protected and Stabilized Gold Clusters. *Bull. Chem. Soc. Jpn.* **2012**, *85*, 151–168.

18 Zhu, M.; Lanni, E.; Garg, N.; Bier, M. E.; Jin, R. Kinetically Controlled, High-Yield Synthesis of Au_{25} Clusters. *J. Am. Chem. Soc.* **2008**, *130*, 1138–1139.

19 Wu, Z.; Suhan, J.; Jin, R. One-Pot Synthesis of Atomically Monodisperse, Thiol-Functionalized Au_{25} Nanoclusters. *J. Mater. Chem.* **2009**, *19*, 622–626.

20 Jin, R.; Qian, H.; Wu, Z.; Zhu, Y.; Zhu, M.; Mohanty, A.; Garg, N. Size Focusing: A Methodology for Synthesizing Atomically Precise Gold Nanoclusters. *J. Phys. Chem. Lett.* **2010**, *1*, 2903–2910.

21 Qian, H.; Zhu, Y.; Jin, R. Atomically Precise Gold Nanocrystal Molecules with Surface Plasmon Resonance. *Proc. Natl. Acad. Sci. U.S.A.* **2012**, *109*, 696–700.

22 Wu, Z.; Gayathri, C.; Gil, R.; Jin, R. Probing the Structure and Charge State of Glutathione-Capped $Au_{25}(SG)_{18}$ Clusters by NMR and Mass Spectrometry. *J. Am. Chem. Soc.* **2009**, *131*, 6535–6542.

23 Shichibu, Y.; Negishi, Y.; Tsukuda, T.; Teranishi, T. Large-Scale Synthesis of Thiolated Au_{25} Clusters via Ligand Exchange Reactions of Phosphine-Stabilized Au_{11} Clusters. *J. Am. Chem. Soc.* **2005**, *127*, 13464–13465.

24 Qian, H.; Eckenhoff, W. T.; Zhu, Y.; Pintauer, T.; Jin, R. Total Structure Determination of Thiolate-Protected Au_{38} Nanoparticles. *J. Am. Chem. Soc.* **2010**, *132*, 8280–8281.

25 Zhu, Y.; Qian, H.; Jin, R. An Atomic-Level Strategy for Unraveling Gold Nanocatalysis from the Perspective of $Au_n(SR)_m$ Nanoclusters. *Chem.—Eur. J.* **2010**, *16*, 11455–11462.

26 Min, B. K.; Friend, C. M. Heterogeneous Gold-Based Catalysis for Green Chemistry: Low-Temperature CO Oxidation and Propene Oxidation. *Chem. Rev.* **2007**, *107*, 2709–2724.

27 Zhu, M.; Eckenhoff, W. T.; Pintauer, T.; Jin, R. Conversion of Anionic $[Au_{25}(SCH_2CH_2Ph)_{18}]^-$ Cluster to Charge Neutral Cluster via Air Oxidation. *J. Phys. Chem. C* **2008**, *112*, 14221–14224.

28 Haruta, M.; Tsubota, S.; Kobayashi, T.; Kageyama, H.; Genet, M. J.; Delmon, B. Low-Temperature Oxidation of CO over Gold Supported on TiO_2, α-Fe_2O_3, and Co_3O_4. *J. Catal.* **1993**, *144*, 175–192.

29 Nie, X.; Qian, H.; Ge, Q.; Xu, H.; Jin, R. CO Oxidation Catalyzed by Oxide-Supported $Au_{25}(SR)_{18}$ Nanoclusters and Identification of Perimeter Sites as Active Centers. *ACS Nano* **2012**, *6*, 6014–6022.

30 Haruta, M. Spiers Memorial Lecture: Role of Perimeter Interfaces in Catalysis by Gold Nanoparticles. *Faraday Discuss.* **2011**, *152*, 11–32.

31 Zhu, Y.; Qian, H.; Zhu, M.; Jin, R. Thiolate-Protected Au_n Nanoclusters as Catalysts for Selective Oxidation and Hydrogenation Processes. *Adv. Mater.* **2010**, *22*, 1915–1920.

32 Liu, Y.; Tsunoyama, H.; Akita, T.; Tsukuda, T. Efficient and Selective Epoxidation of Styrene with TBHP Catalyzed by Au_{25} Clusters on Hydroxyapatite. *Chem. Commun.* **2010**, *46*, 550–552.

33 Jiang, D.-e.; Tiago, M. L.; Luo, W.; Dai, S. The "Staple" Motif: A Key to Stability of Thiolate-Protected Gold Nanoclusters. *J. Am. Chem. Soc.* **2008**, *130*, 2777–2779.

34 Liu, Y.; Tsunoyama, H.; Akita, T.; Xie, S.; Tsukuda, T. Aerobic Oxidation of Cyclohexane Catalyzed by Size-Controlled Au Clusters on Hydroxyapatite: Size Effect in the Sub-2 nm Regime. *ACS Catal.* **2011**, *1*, 2–6.

35 Xie, S.; Tsunoyama, H.; Kurashige, W.; Negishi, Y.; Tsukuda, T. Enhancement in aerobic alcohol oxidation catalysis of Au_{25} clusters by single Pd atom doping. *ACS Catal.* **2012**, *2*, 1519–1523.

36 Zhu, Y.; Qian, H.; Drake, B. A.; Jin, R. Atomically Precise $Au_{25}(SR)_{18}$ Nanoparticles As Catalysts for the Selective Hydrogenation of Alpha,Beta-Unsaturated Ketones and Aldehydes. *Angew. Chem., Int. Ed.* **2010**, *49*, 1295–1298.

37 Yamamoto, H.; Yano, H.; Kouchi, H.; Obora, Y.; Arakawa, R.; Kawasaki, H. N,N-Dimethylformamide-Stabilized Gold Nanoclusters as a Catalyst for the Reduction of 4-Nitrophenol. *Nanoscale* **2012**, *4*, 4148–4154.

38 Shivhare, A.; Ambrose, S. J.; Zhang, H.; Purves, R. W.; Scot, R. W. J. Stable and Recyclable Au_{25} Clusters for the Reduction of 4-Nitrophenol. *Chem. Commun.* **2013**, *49*, 276–278.

39 Sakai, N.; Tatsuma, T. Photovoltaic Properties of Glutathione-Protected Gold Clusters Adsorbed on TiO_2 Electrodes. *Adv. Mater.* **2010**, *22*, 3185–3188.

40 Kogo, A.; Sakai, N.; Tatsuma, T. Photocatalysis of Au_{25}-Modified TiO_2 under Visible and near Infrared Light. *Electrochem. Commun.* **2010**, *12*, 996–999.

41 Kogo, A.; Sakai, N.; Tatsuma, T. Photoelectrochemical Analysis of Size-Dependent Electronic Structures of Gold Clusters Supported on TiO_2. *Nanoscale* **2012**, *4*, 4217–4221.

42 Lee, M.; Amaratunga, P.; Kim, J.; Lee, D. TiO_2 Nanoparticle Photocatalysts Modified with Monolayer-Protected Gold Clusters. *J. Phys. Chem. C* **2010**, *114*, 18366–18371.

43 Chen, W.; Chen, S. Oxygen Electroreduction Catalyzed by Gold Nanoclusters: Strong Core Size Effects. *Angew. Chem., Int. Ed.* **2010**, *48*, 4386–4389.

44 Kumar, S. S.; Kwak, K.; Lee, D. Amperometric Sensing Based on Glutathione Protected Au_{25} Nanoparticles and Their pH Dependent Electrocatalytic Activity. *Electroanalysis* **2011**, *23*, 2116–2124.

45 Kauffman, D. R.; Alfonso, D.; Matranga, C.; Qian, H.; Jin, R. Experimental and Computational Investigation of Au_{25} Clusters and CO_2: A Unique Interaction and Enhanced Electrocatalytic Activity. *J. Am. Chem. Soc.* **2012**, *134*, 10237–10243.

46 Zhu, M.; Qian, H.; Jin, R. Thiolate-Protected $Au_{24}(SC_2H_4Ph)_{20}$ Nanoclusters: Superatoms or Not? *J. Phys. Chem. Lett.* **2010**, *1*, 1003–1007.

47 Zhu, Y.; Wu, Z.; Gayathri, G. C.; Qian, H.; Gil, R. R.; Jin, R. Exploring Stereoselectivity of Au_{25} Nanoparticle Catalyst for Hydrogenation of Cyclic Ketone. *J. Catal.* **2010**, *271*, 155–160.

48 MacDonald, M.; Cheverie, D.; Zhang, P.; Qian, H.; Jin, R. The Structure and Bonding of $Au_{25}(SR)_{18}$ Nanoclusters from EXAFS: The Interplay of Metallic and Molecular Behavior. *J. Phys. Chem. C* **2011**, *115*, 15282–15287.

49 Lopez-Acevedo, O.; Kacprzak, K. A.; Akola, J.; Hakkinen, H. Quantum Size Effects in Ambient CO Oxidation Catalysed by Ligand-Protected Gold Clusters. *Nat. Chem.* **2010**, *2*, 329–334.

50 Pei, Y.; Shao, N.; Gao, Y.; Zeng, X. C. Investigating Active Site of Gold Nanoparticle $Au_{55}(PPh_3)_{12}Cl_6$ in Selective Oxidation. *ACS Nano* **2010**, *4*, 2009–2020.